

Generation and Spectroscopic Characterization of Two Persistent Radical Cations from Bis[4-(dimethylamino)phenyl]squaraine

Lennart Eberson

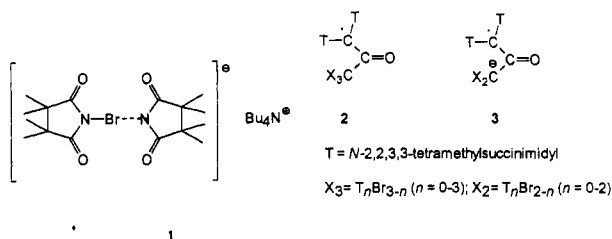
Chemical Center, Lund University, P.O. Box 124, S-221 00 Lund, Sweden

Received: September 13, 1993*

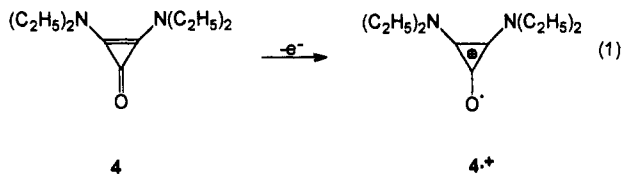
The squaraine dye bis[4-(dimethylamino)phenyl]squaraine gives a persistent radical cation upon one-electron oxidation in dichloromethane. In the presence of trifluoroacetic acid in high concentration (0.5–1.0 M), a second persistent radical cation is detectable upon oxidation, most likely formed by one-electron loss from a dye species protonated on one oxygen and one nitrogen. Both species were characterized by their UV-vis and EPR spectral properties.

I. Introduction

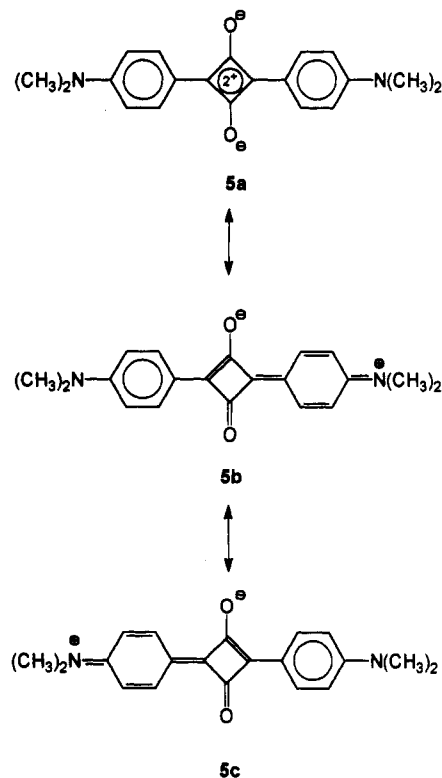
The reaction between acetone and a 1:1 complex of *N*-bromotetramethylsuccinimide and tetrabutylammonium tetramethylsuccinimide¹⁻³ (1) produces a persistent radical with an electron paramagnetic resonance (EPR) spectrum showing coupling to two equivalent nitrogens, in all likelihood with structure 2 or 3.⁴ In connection with this study, we also investigated the



feasibility of structures of cyclopropenone type, using among others 2,3-bis(*N,N*-diethylamino)cyclopropenone (4, $E^\circ[4^{+\bullet}/4] = 0.68$ V vs Ag/AgCl)^{3a} as a model compound.^{3a} Upon oxidation by tris(4-bromophenyl)aminium (TBPA⁺) hexachloroantimonate in acetonitrile, 4 gave a moderately stable radical cation (half-life of 5–10 min at 20 °C; EPR spectral parameters: $a^N(2) = 0.495$ mT, $a^H(8) = 0.81$ mT), as shown in eq 1:



A search for other radical cation structures of similar type as 4⁺ led to dyes of the squaraine family, in this paper represented by the bis(dimethylamino) derivative 5. Squaraine dyes are important photoconductive materials,⁵ this property being related to the redox properties of the dyes, primarily upon oxidation. The electronic structure of 5 is formulated as a bis-oxyanion of the cyclobutadiene dication (5), instead of the classical zwitterionic structures 5a and 5b. This assignment is supported by the fact that no carbonyl stretching frequency is detectable in the infrared spectrum of squaraines,^{6,7} as well as in their NMR spectral behavior.⁸ Compound 5 undergoes two successive, reversible one-electron oxidations at 0.35 and 0.73 V (vs Ag/AgCl), respectively, in dichloromethane/tetrabutylammonium perchlorate, and a large number of other derivatives of 5 had similar electrochemical properties.⁹ The corresponding radical cation, 5⁺, was recently



studied by dynamic methods (flash photolysis, pulse radiolysis) and characterized by its UV spectrum ($\lambda_{\max} = 670$ nm in dichloromethane).¹⁰

In view of the low and reversible redox potential for one-electron oxidation of 5 (compare with that of 4) it was deemed possible that 5⁺ might be generated and studied under static conditions. In what follows, the generation and study by UV-vis and EPR spectroscopy of two persistent radical cations obtained by oxidation of 5 are described.

II. Results

Reactions of 5 upon Oxidation with or without TFA Present. The oxidation of a 3.8 μ M solution (based upon the extinction coefficient of 3.09×10^5 given in ref 10) of 5 in dichloromethane by aliquots of a 0.141 mM solution of TBPA⁺ SbCl₆⁻ in dichloromethane was accompanied by gradual changes in the UV-vis spectrum, as shown in Figure 1. The intense band at 626 nm was replaced by one at 668 nm ($\epsilon \approx 1.97 \times 10^5$, based on a one-electron oxidation), and an EPR spectrum was obtained from the final solution, as shown in Figures 2a and 3a. When this

* Abstract published in *Advance ACS Abstracts*, December 15, 1993.

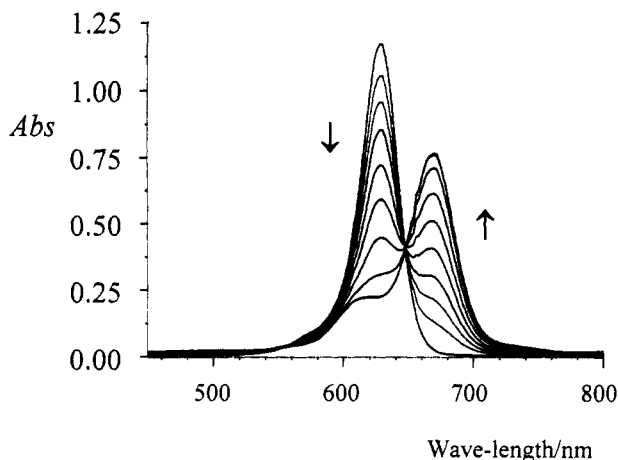


Figure 1. UV-vis spectra of a 3.8 μM solution of **5** in dichloromethane, to which 9.4- μL aliquots of a solution of tris(4-bromophenylaminium) hexachloroantimonate (0.141 mM) in dichloromethane were added incrementally.

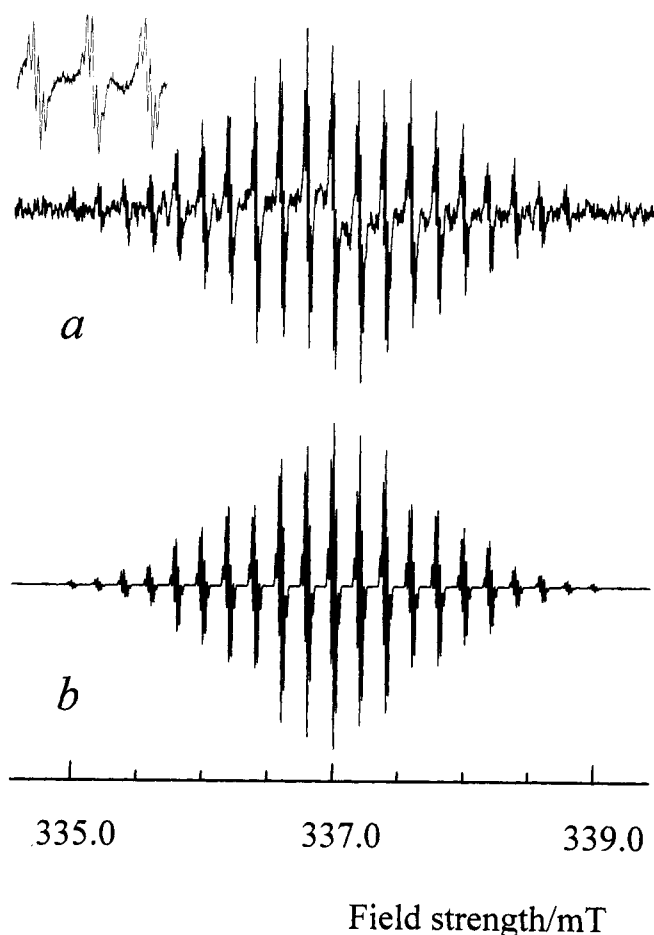


Figure 2. (a) EPR spectrum of the final solution of Figure 1 at 23 $^{\circ}\text{C}$, recorded with a modulation amplitude of 0.016 mT; the inset shows the middle three lines. (b) Simulated spectrum with $a^{\text{N}}(2) = 0.197$, $a^{\text{CH}_3}(12) = 0.39$, and $a^{\text{H}_2}(4) = 0.0186$ mT ($a^{\text{H}_3}(4)$ is assumed to be <0.005 mT), with Gaussian line shape and a line width of 0.014 mT.

solution was left at room temperature, the 668-nm maximum slowly decayed (half-life ~ 10 h). After addition of one redox equivalent of the triarylaminium salt, no spectral changes took place on a time scale of tens of minutes with further addition of the oxidant, except for the growth of the 728-nm maximum of $\text{TBPA}^{+\bullet}$ (Figure 4). The process underlying the spectral evolution in Figure 1 therefore must correspond to the one-electron oxidation of **5**.

The EPR spectrum of Figure 2a was recorded with a low

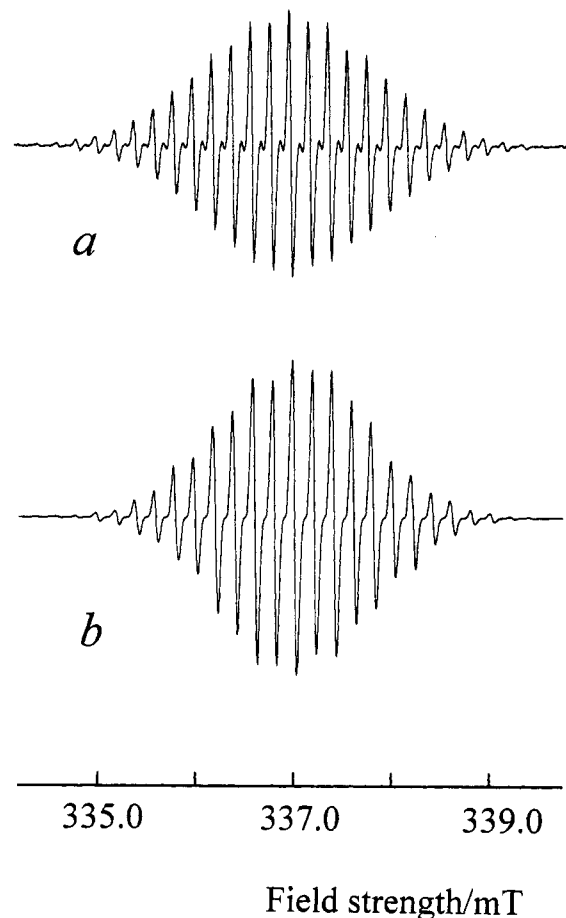


Figure 3. (a) EPR spectrum of the final solution of Figure 1 at 23 $^{\circ}\text{C}$, recorded with a modulation amplitude of 0.051 mT by accumulation of 3000 spectra. (b) Simulated spectrum as in spectrum b of Figure 2, but with a line width of 0.040 mT.

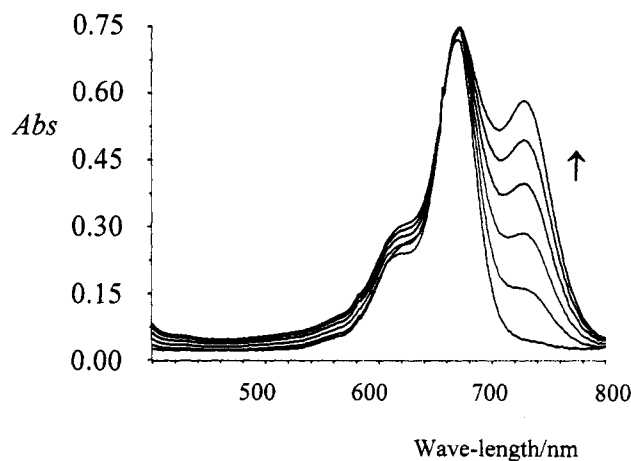


Figure 4. UV-vis spectra of a 3.8 μM solution of **5** in dichloromethane, to which are added aliquots of a solution of $\text{TBPA}^{+\bullet}$. The final solution is $\sim 18 \mu\text{M}$ in $[\text{TBPA}^{+\bullet}]$.

modulation amplitude (0.016 mT) in order to show the small splittings of the main lines (see insert of Figure 2a). With a larger modulation amplitude (0.040 mT), it was possible to detect 29 lines separated by 0.197 mT in the spectrum (Figure 3a).

Since the oxidation of $5^{+\bullet}$ to 5^{2+} occurs at a potential around 1.0 V vs NHE (normal hydrogen electrode)⁹ and $\text{TBPA}^{+\bullet}$ has a redox potential of 1.30 V, it should at least in principle be possible to oxidize $5^{+\bullet}$ to 5^{2+} under the conditions employed. Addition of a 20-fold excess of $\text{TBPA}^{+\bullet}$ to a solution of **5** gave a solution showing initially only the UV-vis spectrum of $5^{+\bullet}$ and $\text{TBPA}^{+\bullet}$. No bands that could be attributed to the formation of 5^{2+} appeared. The decay of $5^{+\bullet}$ was monitored at 626 nm and

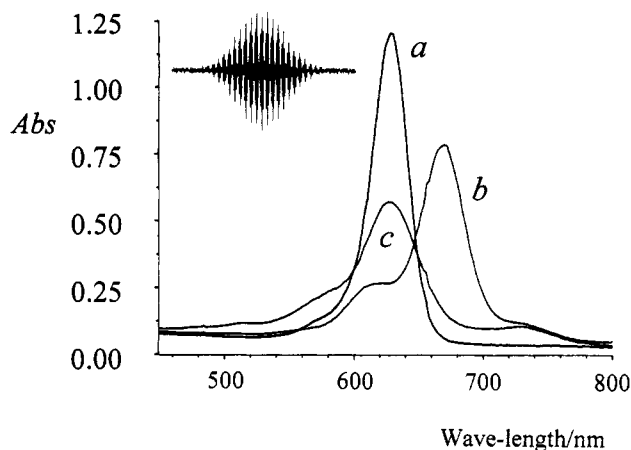


Figure 5. UV-vis spectra of (a) a 3.8 μM solution of **5** in dichloromethane; (b) a 3.8 μM solution of **5** $^{\bullet+}$ in dichloromethane, obtained by TPBA $^{\bullet+}$ oxidation of solution a; and (c) solution b, made 0.4 M in TFA. Inset: EPR spectrum of solution c.

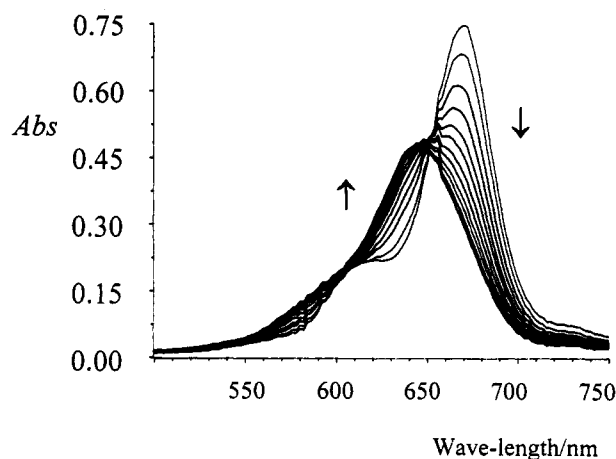


Figure 6. UV-vis spectra of a 3.8 μM solution of **5** $^{\bullet+}$ in dichloromethane, to which TFA was added in ~ 4 mM increments to a final concentration of ~ 40 mM.

followed first-order kinetics with $k = 3.2 \times 10^{-3} \text{ s}^{-1}$ at $[\text{TBPA}^{\bullet+}]_0 = 70 \mu\text{M}$. Runs at several different $[\text{TBPA}^{\bullet+}]_0$ in large excess over $[\text{5}^{\bullet+}]$ indicated approximate first-order dependence upon the former concentration with an average k_2 of $40 \text{ M}^{-1} \text{ s}^{-1}$. During this process, run in an experiment with a 4-fold excess of TBPA $^{\bullet+}$ salt over **5**, the EPR spectrum had the same appearance as in Figure 2a, except for a slight modification due to the presence of TBPA $^{\bullet+}$.

Upon addition of trifluoroacetic acid (0.4 M) to a solution which had been oxidized by one equivalent of TBPA $^{\bullet+}$, the UV-vis spectrum changed drastically (Figure 5): the band with $\lambda_{\text{max}} \approx 668 \text{ nm}$ was replaced by one with $\lambda_{\text{max}} = 628 \text{ nm}$. Incremental addition of TFA in a lower concentration interval gave the spectral changes shown in Figure 6. The final solution (curve c) of Figure 5 exhibited the EPR spectrum shown in the inset of Figure 5. The same spectrum was obtained more cleanly from a more concentrated solution obtained by 2,3-dichloro-5,6-dicyanobenzoquinone (DDQ) oxidation¹¹ of a 0.1 mM solution of **5** in dichloromethane/1.0 M TFA and is shown in Figure 7a. This EPR spectrum was stable over periods of many hours.

Other experiments showed that the EPR spectrum of Figure 2a changed slightly upon addition of TFA in low concentration (up to 35 mM). The splitting between the major lines increased from 0.195 to 0.205 mT, and the quintet splitting of each major line increased to $\sim 0.04 \text{ mT}$.

In order to investigate the effect of acid upon **5**, aliquots of a dilute TFA solution in dichloromethane were added to a solution of **5**. The first process, occurring upon addition of TFA up to

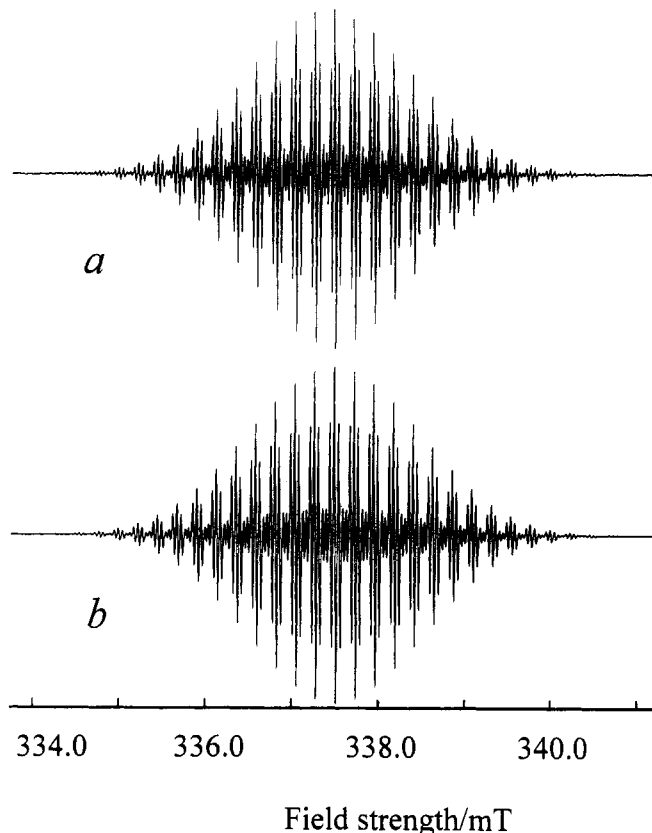


Figure 7. (a) EPR spectrum (modulation amplitude 0.015 mT) of a 0.1 mM solution of **5** in dichloromethane/trifluoroacetic acid (1.0 M), oxidized by DDQ. (b) Simulated spectrum with $a^{\text{N}}(2) = 0.454$, $a^{\text{CH}_3}(12) = 0.454$, $a^{\text{H}_2}(4) = 0.227$, and $a^{\text{H}_3}(4) = 0.047 \text{ mT}$, assuming Gaussian line shape and with a line width of 0.020 mT.

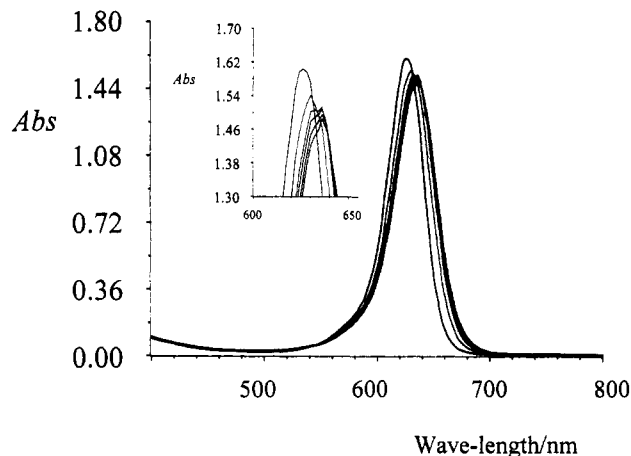


Figure 8. UV-vis spectra of a 5.2 μM solution of **5** in dichloromethane to which 10- μL aliquots of a TFA solution in dichloromethane were added incrementally to a final $[\text{TFA}]$ of 35 mM. Inset: a magnification of the maximum and its changes.

a concentration of $\sim 35 \text{ mM}$, showed only a small effect in the UV spectrum; the 626 nm band moved to 636 nm and decreased slightly in intensity (Figure 8). The final solution was then oxidized by incremental amounts of TBPA $^{\bullet+}$ and behaved in the same way as shown in Figure 1; the 636-nm band disappeared and was replaced by the 668-nm band. The EPR spectrum of the oxidized solution was the same as that shown in Figure 2a, modified by addition of $\sim 35 \text{ mM}$ TFA.

When TFA was added to the solution of **5** in dichloromethane, again in incremental fashion but now up to a final concentration of $\sim 450 \text{ mM}$, the spectrum underwent a major change (Figure 9), with at least three new bands appearing in the 450–550-nm region along with the disappearance of the 636-nm band. The

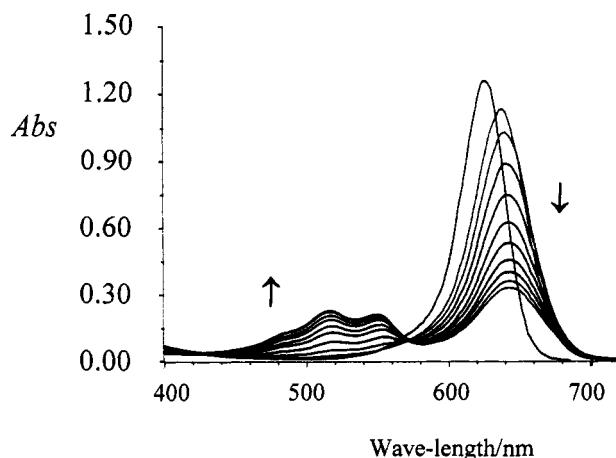
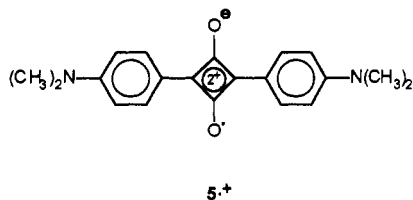


Figure 9. UV-vis spectra of a 4.2 μM solution of **5** in dichloromethane to which 10- μL aliquots of TFA were added incrementally to a final [TFA] of 0.45 M.

final solution upon oxidation by TBPA^{++} produced the same EPR spectrum as that in Figure 7a.

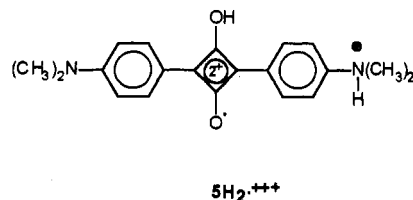
III. Discussion

Assignment and Analysis of the EPR Spectra. In the analysis to follow, it is assumed that the structure of **5** is best represented by the cyclobutandienediyl structure. Since the UV spectra of the solutions exhibiting the EPR spectra of Figures 2a, 3a, and 7 were distinctly different (see Figure 4), the EPR spectra must correspond to different species and not merely reflect possible dynamic processes, like electron exchange between a radical cation and its parent. Most likely the appearance of two species is connected with the acid-base chemistry of **5**. The species corresponding to the EPR spectra of Figures 2a and 3a must then correspond to the radical cation of **5** ($5^{\bullet+}$), since no acid had been added in this experiment.



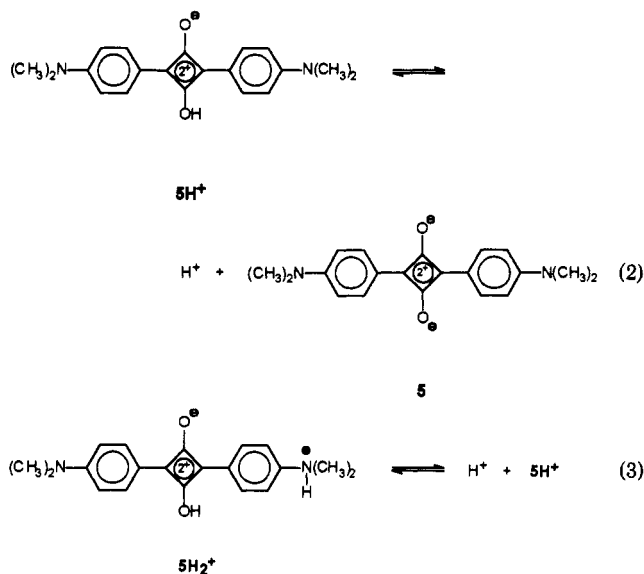
Its UV-vis spectral maximum at 668 nm agrees well with that reported from dynamic studies, 670 nm.¹⁰ The spectrum of Figure 2a showed 29 major lines with spacing 0.197 mT, each split into a quintet with a hyperfine splitting (hfs) constant of 0.0186 mT. The best stimulation of the spectrum was obtained using the following hfs's: $a^{\text{N}}(2) = 0.197$, $a^{\text{CH}_3}(12) = 0.400$, and $a^{\text{H}^2}(4) = 0.0186$ mT, with negligible coupling to the H3 hydrogens, assuming Gaussian line shape and with a line width of 0.014 mT (Figure 2b). With a line width of 0.04 mT, this set of parameters gives a spectral simulation with 29 major lines of spacing 0.197 mT (Figure 3b).

The second EPR spectrum (inset of Figure 5, Figure 7a) must originate from a protonated species where protonation has strongly influenced the conjugation in the squaraine molecule, as judged by the series of UV-vis spectra of Figure 9 (see also the spectral changes in Figure 5). It is likely that this species is the radical cation of bisprotonated **5**, $5\text{H}_2^{\bullet+}$, where one oxygen and one of the nitrogens are protonated, the latter process leading to a break in the conjugation between the nitrogen and the four-membered ring.



Moreover, since $5\text{H}_2^{\bullet+}$ must be a fairly strong acid (see below) and is present in an acidic medium, the proton exchange at the nitrogen must be fast, and the EPR spectrum should correspond to a species with averaged nitrogen and hydrogen atoms. Thus the EPR spectrum of Figure 7a was best simulated by the following set of hfs's: $a^{\text{N}}(2) = 0.454$, $a^{\text{CH}_3}(12) = 0.454$, $a^{\text{H}^2}(4) = 0.227$, and $a^{\text{H}^3}(4) = 0.047$ mT, assuming Gaussian line shape and with a line width of 0.025 mT (Figure 7b). It was possible to detect experimentally all 39 of the 39 theoretically possible major groups of lines.

Acid-Base Chemistry of 5 and Its Connection with the Spectroscopic Results. Little is known about the acid-base properties of squaraine dyes. The first pK_a of a squarylium dye (determined¹² for a bis(benzothiazolium) derivative) is 3.6 ± 0.5 and in this case must correspond to the deprotonation of the *O*-protonated form of the dye molecule, *i.e.*, eq 2 in the case of **5**. The second site of protonation most likely is one of the nitrogens (eq 3), since in **5** this is located in an *N,N*-dimethylaniline, substituted in the 4-position by a strong electron acceptor.



The first of these protonation processes should not significantly affect the conjugation in the dye molecule, and thus the UV-vis spectrum only undergoes minor changes (Figure 8) upon addition of TFA up to a concentration of 35 mM. The same should apply to the EPR spectrum. Thus the radical species observed in this region of acidity should be $5^{\bullet+}$ (Figures 2a and 3a), possibly in fast equilibrium with the corresponding *O*-protonated species, like 5H^{2+} in the presence of TFA in low concentration.

The addition of TFA in higher concentrations leads to additional protonation at one of the nitrogens, thus impeding conjugation in the molecule. This factor changes the UV-vis spectrum of **5** drastically (Figure 9), in that several new bands at lower wavelengths appear and the 636-nm band almost disappears. The radical cation species obtained by oxidation of this solution ($5\text{H}_2^{\bullet+}$) has a different UV-vis spectrum from that of $5^{\bullet+}$ (Figure 5 vs Figure 1) and is characterized by carrying more spin density on nitrogen and ring and methyl hydrogens according to its EPR spectrum (Figure 7a).

Experimental Section

Materials. The preparation of **5** was carried out as described.¹³ Tris(4-bromophenyl)aminium hexachloroantimonate was from Aldrich, and its solutions were calibrated spectrophotometrically immediately before use.¹⁴ Trifluoroacetic acid and dichloromethane were of UVASOL quality (Merck AG).

Instrumentation. UV-vis spectra were recorded by an HP-8452A diode array spectrophotometer, equipped with the HP-89532A and 89532K software. EPR spectra were obtained by the Upgrade Version ESP 3220-200SH of the Bruker ER-200D spectrometer.

Acknowledgment. Financial support from the Swedish Natural Science Research Council and the Knut and Alice Wallenberg Foundation is gratefully acknowledged.

References and Notes

- (1) Barry, J. E.; Finkelstein, M.; Moore, W. M.; Eberson, L. *Tetrahedron Lett.* **1984**, 2847.
- (2) Elding, M.; Albertsson, J.; Svensson, C.; Eberson, L. *Acta Chem. Scand.* **1990**, *44*, 135.
- (3) (a) Eberson, L.; Kubacek, P. *Acta Chem. Scand.* **1990**, *44*, 384. (b) Eberson, L. *Pure Appl. Chem.* **1991**, *63*, 205.
- (4) Eberson, L.; Kubacek, P. *Acta Chem. Scand.* **1992**, *46*, 496.
- (5) Law, K.-Y. *Chem. Rev.* **1993**, *93*, 449.
- (6) Sprenger, H.-E.; Ziegenbein, W. *Angew. Chem.* **1968**, *80*, 541.
- (7) Law, K.-Y.; Bailey, F. C.; Bluett, L. J. *Can. J. Chem.* **1986**, *64*, 1607.
- (8) Law, K.-Y. *J. Phys. Chem.* **1989**, *93*, 5925.
- (9) Law, K.-Y.; Facci, J. S.; Bailey, J. S.; Yanus, J. F. *J. Imag. Sci.* **1990**, *34*, 31.
- (10) Kamat, P. V.; Das, S.; Thomas, K. G.; George, M. V. *J. Phys. Chem.* **1992**, *96*, 195.
- (11) Handoo, K. L.; Gadru, K. *Curr. Sci.* **1986**, *55*, 920.
- (12) Piechowski, A. P.; Bird, G. R.; Morel, D. L.; Stogryn, E. L. *J. Phys. Chem.* **1984**, *88*, 934.
- (13) Sprenger, H.-E.; Ziegenbein, W. *Angew. Chem.* **1966**, *78*, 937.
- (14) Eberson, L.; Larsson, B. *Acta Chem. Scand., Ser. B* **1986**, *40*, 210.